



Available online at
ScienceDirect
 www.sciencedirect.com

Elsevier Masson France
EM|consulte
 www.em-consulte.com



Original Article

Differentiation of tumor progression from pseudoprogression in glioblastoma patients with GRASP DCE-MRI and DSC-MRI



Vichyat Var^{b,c,1}, Severina M. Leu^{b,d,1}, Nikki Rommers^{b,e}, Marios N. Psychogios^{b,c},
 Dominik Cordier^{b,d,2}, Ramona A. Todea^{a,b,c,2,*}

^a Department of Neuroradiology, University Hospital Zurich, Rämistrasse 100, CH-8091, Zurich, Switzerland

^b University of Basel, Petersplatz 1, 4001, Basel, Switzerland

^c Division of Neuroradiology, Clinic of Radiology and Nuclear Medicine, University Hospital of Basel, Petersgraben 4, 4031, Basel, Switzerland

^d Clinic of Neurosurgery, University Hospital of Basel, Spitalstrasse 21, 4031, Basel, Switzerland

^e Department of clinical research, University Hospital of Basel, Spitalstrasse 8/12, 4031, Basel, Switzerland

ARTICLE INFO

Keywords:

Glioblastoma

Progressive disease

Pseudoprogression

Multiparametric analysis, DSC-MRI, DCE-MRI

ABSTRACT

Purpose: This study investigates the diagnostic accuracy of combined Golden Angle Radial Sparse Parallel Dynamic contrast-enhanced (GRASP DCE-) and Dynamic susceptibility contrast (DSC) MRI in differentiating PD from PsP following RCT in differentiating progressive disease (PD) from pseudoprogression (PsP) following radiochemotherapy (RCT) in glioblastoma patients.

Materials and methods: This retrospective study included glioblastoma patients who underwent surgery and RCT between 2017 and 2021 and developed contrast-enhancing lesions suspicious for PD or PsP and had GRASP DCE- and DSC-MRI. Diagnostic accuracy of perfusion parameters was evaluated using the area under the receiver operating characteristics curve (AUC) at both initial suspicion of progression and confirmation MRI.

Results: Among 83 patients, 62 were classified as PD and 21 as PsP on serial MRI for all patients, with additional histological confirmation in 18 patients. Median perfusion parameters values were higher in the PD group in comparison to the PsP group (rCBV: 3.48 vs. 1.60, $p < .001$; Vp: 0.08 vs. 0.05, $p = .032$). At initial suspicion of progression, the combination of Ktrans, Ve, Vp and rCBV improved diagnostic accuracy in differentiating PD from PsP (AUC = 0.77, 95 % CI [0.62–0.93]) compared to rCBV alone (AUC = 0.69, 95 % CI [0.54–0.85]). At confirmation MRI (>12 weeks post-RCT), the added value of DCE was more modest (AUC improvement from 0.88 to 0.90). Suggested optimal thresholds at confirmation were: rCBV 2.87 (Sensitivity 71 %, Specificity 94 %), Ktrans 0.12 min^{-1} (73 %, 76 %), Ve 0.31 (75 %, 65 %), and Vp 0.05 (78 %, 59 %).

Conclusion: Combining DCE- with DSC-MRI may enhance diagnostic accuracy in distinguishing progressive disease from pseudoprogression in glioblastoma, particularly during the early post-radiochemotherapy phase when treatment decisions are critical. As the added value of DCE-MRI is limited beyond 12 weeks post-radiochemotherapy, the full protocol is best reserved for early suspicion of progression or unclear cases, while DSC-MRI alone may be sufficient for confirmation imaging after this period.

Introduction

Glioblastoma is the most common primary malignant brain tumor in adults^{1–3} with a median survival of 15–18 months.⁴ The standard treatment consists of maximal safe resection followed by radio-chemotherapy

(RCT) with Temozolomide®.⁵ Up to 30 % of patients showing *O6-methylguanine-methyltransferase* promoter methylation may develop new or increasing contrast-enhancing lesions due to an inflammatory response enhanced by the alkylating effects of Temozolomide®. This phenomenon, termed pseudoprogression (PsP), is more prevalent within 12

Abbreviations: GRASP DCE-MRI, Golden Angle Radial Sparse Parallel Dynamic Contrast-Enhanced MRI; Ktrans, Volume transfer constant between intravascular and extravascular extracellular space; PD, Progressive disease; PsP, Pseudoprogression; RANO, Response assessment in neuro-oncology; RCT, Radiochemotherapy; sRes, Spatial resolution; tRes, Temporal resolution; Vp, Fractional plasma volume; Ve, Fractional volume of the extravascular extracellular space

* Corresponding author: Senior consultant, Department of Neuroradiology, University Hospital Zurich, Rämistrasse 100, CH-8091, Zurich, Switzerland.

E-mail addresses: severina.leu@usb.ch (S.M. Leu), Nikki.Rommers@usb.ch (N. Rommers), marios.psychogios@usb.ch (M.N. Psychogios), domink.cordier@usb.ch (D. Cordier), ramona.todea@usz.ch (R.A. Todea).

Manuscript type: Original research.

¹ Co-shared first authorship: Vichyat Var, Severina Maria Leu MD.

² Co-shared senior authorship: Dominik Cordier MD Prof., Ramona-Alexandra Todea MD.

<https://doi.org/10.1016/j.neurad.2025.101354>

Available online 24 May 2025

0150-9861/© 2025 The Authors. Published by Elsevier Masson SAS. This is an open access article under the CC BY license (<http://creativecommons.org/licenses/by/4.0/>)

weeks after completion of RCT – a time window in which the response assessment in neuro-oncology (RANO) 2.0 criteria⁶ struggle to distinguish PsP from tumor progression (PD).^{7,8} PsP mistaken for PD may result in the discontinuation of an effective therapy, while PD mistaken for PsP may lead to the continuation of an ineffective therapy with further tumor growth. In contrast to PD, PsP is not associated with neoangiogenesis and this difference may be explored with perfusion MRI.⁹

The most used perfusion techniques DSC-MRI and DCE-MRI are monitoring the contrast agent concentration through fast repeated acquisitions of images of the same tissue volume before and during the contrast-agent passage through the tissue.^{10, 11} DSC-MRI is more commonly used due to its rapid acquisition times, straightforward postprocessing, and widespread availability.^{12,13} It allows the assessment of the neoangiogenesis through rCBV.¹⁴⁻¹⁶ However, the measurement of rCBV might be hindered by the presence of susceptibility artifacts and the effects of contrast leakage.^{12,17} DCE-MRI could complement DSC-MRI since it is less influenced by susceptibility artifacts and it assesses both tissue perfusion and the blood-brain-barrier (BBB) permeability through Ktrans (volume transfer constant), Vp (fractional plasma volume), and Ve (fractional volume of the extravascular extracellular space). For an accurate estimation of the permeability parameters, DCE-MRI requires an optimized protocol for the highest achievable SNR with simultaneous high spatial resolution (sRes) and temporal resolution (tRes).^{18,19} Conventional DCE-MRI commonly restricts tRes while enabling higher sRes for dynamic imaging which yields data unsuitable for pharmacokinetic modelling with inaccurate estimation of the parameters.¹⁸ Fast acquisition strategies with undersampled k-space like Golden Angle Radial Sparse Parallel (GRASP) offer simultaneously high sRes and tRes²⁰⁻²³ and could be added to the more commonly acquired DSC-MRI in a double perfusion-protocol with acceptable acquisition time for the clinical flow.²⁴

The aim of this study is to determine the diagnostic accuracy of combined GRASP DCE-MRI and DSC-MRI in differentiating PD from PsP in glioblastoma patients.

Materials and methods

Study design

The study was approved by the ethics committee. All participants had written or waived informed consent. We performed a retrospective monocentric study between 01/2017 - 12/2021 of patients with histopathologic diagnosis of glioblastoma. The inclusion criteria were: (1) adult patients who underwent (2) surgery and postoperative RCT, (3) had contrast-enhanced (CE) postoperative MRI within 24 h, (4) developed new or enlarging CE lesions $\geq 10 \times 10$ mm, (5) had CE confirmation MRI ≥ 12 weeks after completion of RCT as confirmation scan for PD or PsP, and (6) had GRASP DCE-MRI and DSC-MRI sequences. The exclusion criteria were: (1) missing consent, (2) incomplete MRI follow-up, (3) death prior to completion of therapy, or (4) stable disease (Fig. 1). Study data were managed using the Research Electronic Data Capture (REDCap) software.²⁵

Imaging protocol

All MRI scans were performed with a 3T scanner (MAGNETOM Skyra, Siemens Healthineers) with a 20-channel head-neck coil. Contrast material: 20 ml Gadoteracid (0.5 mmol/ml, Dotarem® Guerbet), via 20 G iv catheter.

For the RANO 2.0 assessment T1-weighted post-contrast sequences were used. The dynamic sequences were acquired in one protocol with a split-bolus technique where the first contrast bolus injected for the GRASP DCE-MRI served as preload to correct for T1-weighted leakage effects in the consecutive DSC-MRI acquisition, with the purpose to avoid the underestimation of rCBV.²⁴ Initially, a 25 mL intravenous injection of NaCl (0.9 % saline) is administered prior to the contrast agent. Baseline acquisition of the GRASP DCE-MRI sequence is

performed for 20 s. Following this, 10 mL of Gadoteracid is injected at a rate of 2 mL/s[12], and dynamic DCE-MRI acquisition is conducted for a total duration of 4:23 min. Subsequently, a 25 mL NaCl bolus is injected, and baseline acquisition of DSC-MRI is performed for 15 s. The second dose of Gadoteracid (10 mL) is then administered at a rate of 5 mL/s, with dynamic DSC-MRI acquisition continuing for 2:96 min. Finally, 30 mL of NaCl is reinjected to complete the protocol.

GRASP DCE-MRI uses a continuous acquisition of k-space with the following parameters: TR 4.09 ms, TE 1.92 ms, flip angle 12°, FOV 240 mm, matrix size 256 × 256, voxel size 1.5-mm isotropic, radial views 850, slice partial Fourier 6/8, bandwidth 400Hz/pixel, 4:23 min total acquisition. The dynamic images were reconstructed with a tRes of 4.3 s.²⁶

DSC-MRI was acquired using a T2*-weighted gradient-echo single-shot echoplanar imaging sequence with GRAPPA acceleration and motion correction. The sequence parameters included: TR 2000 ms, TE 35 ms, flip angle 60°, FOV 230 mm, matrix size 128 × 128 mm, slice thickness 6 mm; voxel size 1.8 mm × 1.8 mm × 6.0 mm, bandwidth 1446 Hz/pixel; acquisition time 2:96 min.

Imaging analysis

One board-certified neuroradiologist Reader 1 (10 years of experience in radiology, 5 years in neuroradiology) assigned the 83 patients to the PD (n=62) or PsP group (n=21) according to the RANO 2.0 criteria⁶ and the CE lesion outcome based on serial MRI, histology, or O-(2-[18F]fluoroethyl)-L-tyrosine PET (FET-PET CT) (detailed description in the Supplementary material).

The postprocessing of perfusion studies was done with Olea Sphere v3.0 (Olea Medical SAS, La Ciotat, France) by Reader 1 and Reader 2 (Radiology resident “in training”), both blinded to the lesion outcome at the time of the measurements. The parameters were extracted from GRASP DCE-MRI using a two-compartment extended Tofts model with automated arterial input function at the level of the ICA. For the DSC-MRI analysis, an arterial input function and a correction for contrast-agent leakage to extra-vascular space through the estimation of a leakage parameter (K2) were used.²⁷

The mean rCBV, Ktrans, Ve, and Vp were measured in two manually defined ROIs (20–30mm²) at the level of the “hotspot” in the color-coded maps. When measuring rCBV, areas with magnetic susceptibility artifacts were avoided, and normalization was achieved by placing a third ROI in normal appearing white matter of the centrum semiovale on the contralateral side.

All perfusion studies were analyzed at the initial suspicion of progression “PD/PsP suspicion MRI” and at then at the confirmation scan “PD/PsP confirmation MRI”. According to the RANO 2.0 criteria all new lesions outside the irradiated volume, that appeared within 12 weeks after completion of RCT were considered PD, and the suspicion scan coincided with the confirmation scan. For all other lesions location within the irradiated volume, multiple follow-ups were available. The confirmation scan was assigned as the first MRI performed after the 12 weeks after completion of RCT.

Statistical analysis

The comparison of perfusion parameters between groups was performed using the Wilcoxon signed-rank test. A logistic regression model with progression (PsP vs. PD) as the outcome and each of the perfusion variables as a single predictor, as well as with all four parameters combined (in an additive way in a logistic regression model) was fitted. The Area under the Curve (AUC) of the Receiver-Operator Characteristics (ROC) curve with its 95 % confidence interval (CI) (according to DeLong’s method to define the variance of the AUC) was used to evaluate the accuracy of the perfusion parameters to differentiate PD from PsP.²⁸ Furthermore, sensitivity and specificity were calculated with bootstrap resampling and averaging methods by Fawcett.²⁹ The accuracy for the best cut-off was calculated with 95 % CI according to

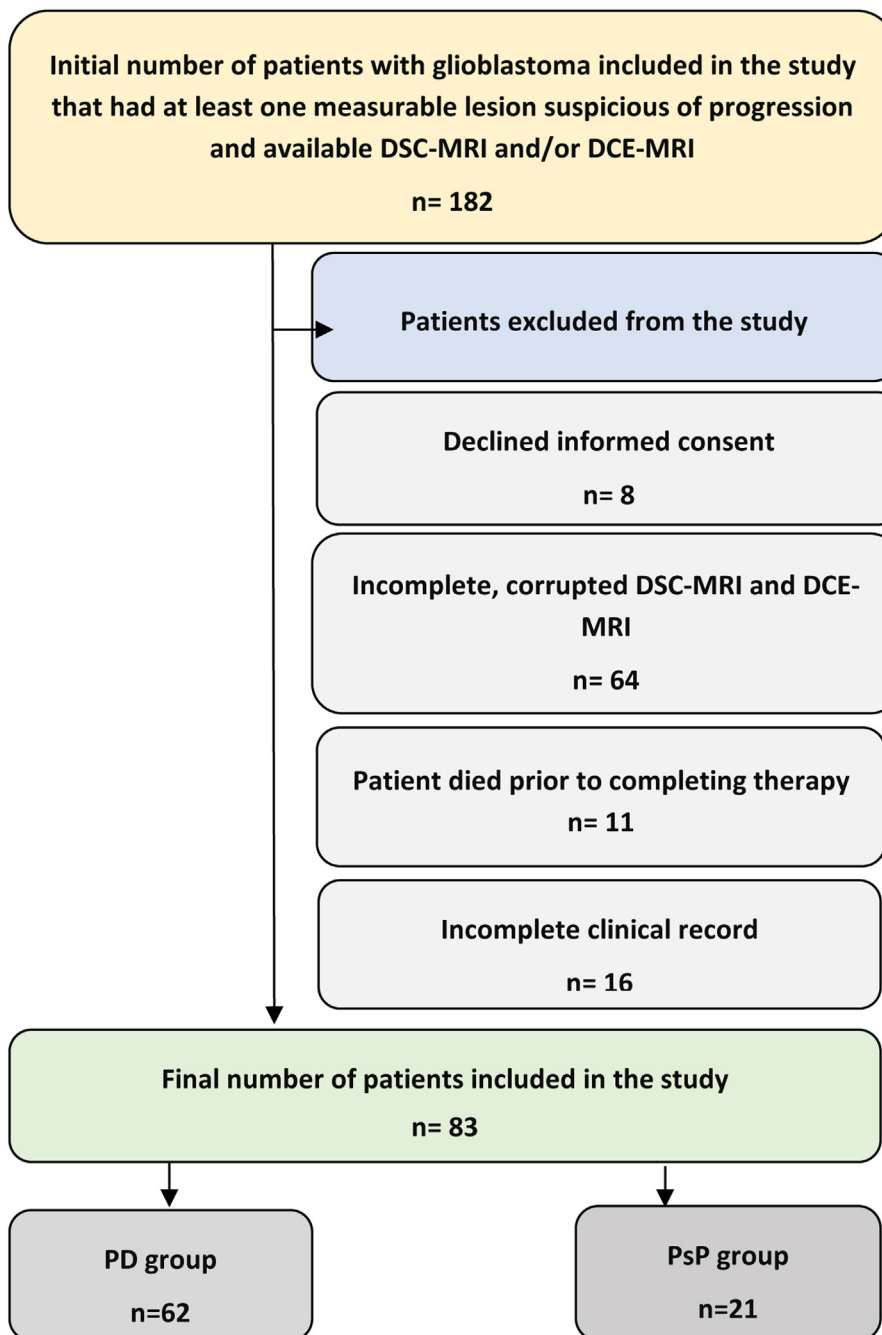


Fig. 1. Flow diagram of the patients included in the study.

Blaker.³⁰ The correct classification of PD patients was considered of higher importance, and minimum sensitivity of 60 % was required in the determination of the cut-off value. As a sensitivity analysis, we performed a leave-one-out cross validation for which we calculated the AUC with corresponding percentile confidence interval.^{28, 31}

A reliability analysis was conducted between the two readers, and the intraclass correlation coefficient (ICC) was calculated for both DSC- and DCE-MRI parameters. All statistical analyses were performed in R.³² “This article follows the STARD reporting guidelines.”

Results

Baseline characteristics of the patients and analysis sets

83 patients fulfilled the inclusion criteria. They had a mean age of 59 ± 14 years, and 54 of them were men. The *O6-methylguanine-*

methyltransferase promoter was unmethylated in 43 of 83 patients (37 patients with PD, 6 patients with PsP). 62 patients were included in the PD-group, and 21 in the PsP-group. The lesion outcome (PD vs. PsP) was established on serial MRI for all 83 patients. 18 patients also had surgery and the PD (n=16) or PsP (absence of vital tumor, n=2) was confirmed with histology. 2 additional patients (one with PD and the other with PsP) had also a FET-PET/CT that was used to establish lesion outcome (Fig. 1 and Table 1).

In total, 161 perfusion studies were available. All patients had an MRI at the initial suspicion of progression (“PD/PsP suspicion MRI”, n=83 perfusion studies). For 12 patients the initial scan coincided with the confirmation scan because the patients had a progressive disease represented by a new lesion outside the irradiated volume of brain. In total, 78 scans were considered “PsP/PD confirmation scans”, knowing that some patients had more than one MRI follow-up to confirm the progression.

Table 1
Baseline characteristics of the patients.

Characteristic	Total (n = 83)	PsP group (n = 21)	PD group (n = 62)
Mean age (SD)	59.23 (13.7)	59.44 (10.09)	59.42 (14.28)
Gender - M (%)	54 (64.6)	13 (61.9)	41 (67.8)
Glioblastoma integrated diagnosis	83	21	62
MGMT promotor methylation status – unmethylated	43	6	37
Operation type (nr. of patients)			
Biopsy	8	3	5
Complete Resection (complete resection of the contrast-enhancing tumor)	31	6	25
Partial Resection	44	12	32
Re-Resection	18	2	16
PD or PsP confirmation method (note: more than on possible)			
MRI serial follow-up	83	21	62
Surgery/Histology (MRI confirmation and resection)	18	2	16
PET-CT (MRI confirmation and PET)	2	1	1
Progression free survival in days (SD)		101.5 [81.5–131.5]	110.0 [26.5–205.0]

Table 2

Median values [IQR] of the perfusion parameters extracted from DSC-MRI and GRASP DCE-MRI in the PD and PsP group at the first PD/PsP suspicion and at the PD/PsP confirmation.

PD/PsP suspicion MRI	PsP group	PD group	p value
rCBV	2.13 [1.63–2.81]	3.28 [2.27–4.31]	0.02
Ktrans	0.13 [0.09–0.17]	0.15 [0.09–0.36]	0.252
Ve	0.36 [0.23–0.50]	0.39 [0.28–0.64]	0.195
Vp	0.06 [0.04–0.08]	0.07 [0.06–0.11]	0.088
PD/PSP confirmation MRI			
rCBV	1.60 [1.33–2.27]	3.48 [2.49–4.84]	<0.001
Ktrans	0.09 [0.07–0.12]	0.14 [0.11–0.30]	0.002
Ve	0.30 [0.20–0.39]	0.43 [0.31–0.62]	0.015
Vp	0.05 [0.04–0.08]	0.08 [0.06–0.12]	0.032

Group comparisons between PD and PsP

The median values of the perfusion parameters were generally higher in the PD group in comparison to the PsP group with rCBV (PD: 3.48 [2.49–4.84], PsP: 1.6 [1.33–2.27], $p < 0.001$) and Vp (PD: 0.08 [0.06–0.12], PsP: 0.05 [0.04–0.08], $p = .032$) showing statistically significant differences between groups (Table 2).

Diagnostic accuracy of the DSC-MRI (rCBV) and DCE-MRI (Ktrans, Vp, Ve) parameters to differentiate progressive disease from pseudoprogression after completion of RCT

At the initial suspicion of progression (PD/PsP suspicion MRI), the combined multiparametric analysis (rCBV, Ktrans, Ve, and Vp) demonstrated higher accuracy (AUC = 0.77, 95 % CI [0.62, 0.93], sensitivity 83 %, specificity 71 %) in differentiating PD from PsP, compared to rCBV alone (AUC = 0.69, 95 % CI [0.54, 0.85], sensitivity 70 %, specificity 73 %). (Table 3).

At the confirmation MRI, after 12 weeks post-RCT, the addition of DCE-MRI improved further the diagnostic accuracy (AUC = 0.90, 95 % CI [0.82, 0.98], sensitivity 78 %, specificity 100 %) compared to rCBV (AUC = 0.88, 95 % CI [0.80, 0.97], sensitivity 71 %, specificity 94 %) (Table 3).

The perfusion parameters showed higher diagnostic accuracy at the confirmation MRI, with the following thresholds: Ktrans 0.12 min⁻¹ (AUC = 0.75, 95 % CI [0.61, 0.89], sensitivity 73 %, specificity 76 %); Ve 0.31 (AUC = 0.69, 95 % CI [0.53, 0.85], sensitivity 75 %, specificity 65 %); and Vp 0.05 (AUC = 0.68, 95 % CI [0.52, 0.84], sensitivity 78 %, specificity 59 %) with rCBV showing the highest accuracy as an individual parameter (threshold: 2.87, AUC = 0.88, 95 % CI [0.80, 0.97], sensitivity 71 %, specificity 94 %) (Table 3 and Figs. 2 and 3).

The results of the leave-one-out cross-validation for each individual perfusion parameter threshold as well as the AUC were equal or very close to those in the main analysis. In consequence, the results of the main analysis were accepted as valuable (Table 4).

An ICC analysis was performed between two readers and the results were as follows: ktrans: 0.79 (excellent reliability), Ve: 0.70 (good reliability), rCBV: 0.40 (fair reliability), and Vp: 0.02 (poor reliability).

Discussion

After completion of postoperative radiochemotherapy, distinguishing progressive disease from pseudoprogression remains challenging on standard sequences, and the current RANO 2.0 criteria struggle to perform this differentiation.^{6, 33, 34} This distinction is crucial since PD mistaken for PsP may lead to continuation of an ineffective therapy with consequent tumor growth, while PsP mistaken for PD may lead to discontinuation of effective therapy.

The aim of this study is to determine the diagnostic accuracy of a double perfusion study encompassing Golden Angle Radial Sparse Parallel (GRASP) DCE-MRI combined with DSC-MRI in differentiating PD from PsP in glioblastoma patients following RCT.

This study demonstrates that adding DCE-MRI-derived permeability parameters (Ktrans, Vp, and Ve) to the commonly used DSC-MRI parameter rCBV enhances diagnostic accuracy in differentiating PD from PsP, both at the time of suspicion and confirmation MRIs. The benefit is particularly significant during the early post-radiochemotherapy phase, at the initial suspicion of progression—an especially critical period when decisions about transitioning from first-line to second-line therapy are made. At this stage, the combined multiparametric analysis achieved higher diagnostic accuracy (AUC = 0.77, 95 % CI [0.62, 0.93]) compared to rCBV alone (AUC = 0.69, 95 % CI [0.54, 0.85]). Although DCE-MRI continued to improve diagnostic accuracy at the confirmation MRI after 12 weeks post-RCT, the added benefit was more modest (AUC increased from 0.88 to 0.90).

While DSC-MRI is more often used in the clinical routine due to its rapid acquisition times, straightforward postprocessing, and widespread availability,^{12, 13} the measurement of rCBV might be hindered by the presence of susceptibility artifacts due to hemorrhage and the contrast leakage effects.^{12,17} DCE-MRI could complement DSC-MRI since it is less influenced by susceptibility artifacts and it provides additional information on tissue perfusion and BBB permeability.

Given that suspicion of progression in glioblastoma is common within 12 weeks after radiochemotherapy, a period when the incidence of PsP overlaps with PD, combining both DCE- and DSC-MRI may increase radiologist confidence in assessing lesions that typically contain a mix of tumor and radionecrotic tissue. DCE-MRI not only enables a multiparametric analysis using a pharmacokinetic model as mentioned

Table 3
Diagnostic accuracy with 95 % confidence interval of perfusion parameters best thresholds to distinguish PD and PsP at the of PD/PsP suspicion MRI and at PD/PsP confirmation MRI.

Parameter	AUC	Threshold	Sensitivity	Specificity	Accuracy
At PD/PsP suspicion MRI					
rCBV	0.69 [0.54, 0.85]	2.45	70 [56, 82]	73 [53, 93]	70.8 [59, 81]
Ktrans	0.59 [0.44, 0.74]	0.11	66 [52, 79]	44 [19, 70]	60 [47, 72]
Vp	0.64 [0.47, 0.81]	0.05	82 [70, 93]	50 [25, 75]	73[61, 84]
Ve	0.60 [0.45, 0.76]	0.24	79 [66, 91]	35 [12, 60]	67[54, 78]
All parameters combined (rCBV, Ktrans,Ve,Vp)	0.77 [0.62, 0.93]		83 [72, 95]	71 [46, 93]	80 [70, 91]
At PD/PsP confirmation MRI					
rCBV	0.88 [0.80, 0.97]	2.87	71 [56, 85]	94 [81, 100]	76 [64, 86]
Ktrans	0.75 [0.61, 0.89]	0.12	73 [58, 83]	76 [59, 94]	74 [61, 83]
Vp	0.68 [0.52, 0.84]	0.05	78 [69, 90]	59 [35, 82]	73 [61, 83]
Ve	0.69 [0.53, 0.85]	0.31	75 [63, 88]	65 [41, 88]	72 [60, 82]
All parameters combined (rCBV, Ktrans,Ve,Vp)	0.90 [0.82, 0.98]		78 [64, 91]	100 [100, 100]	84 [75, 94]

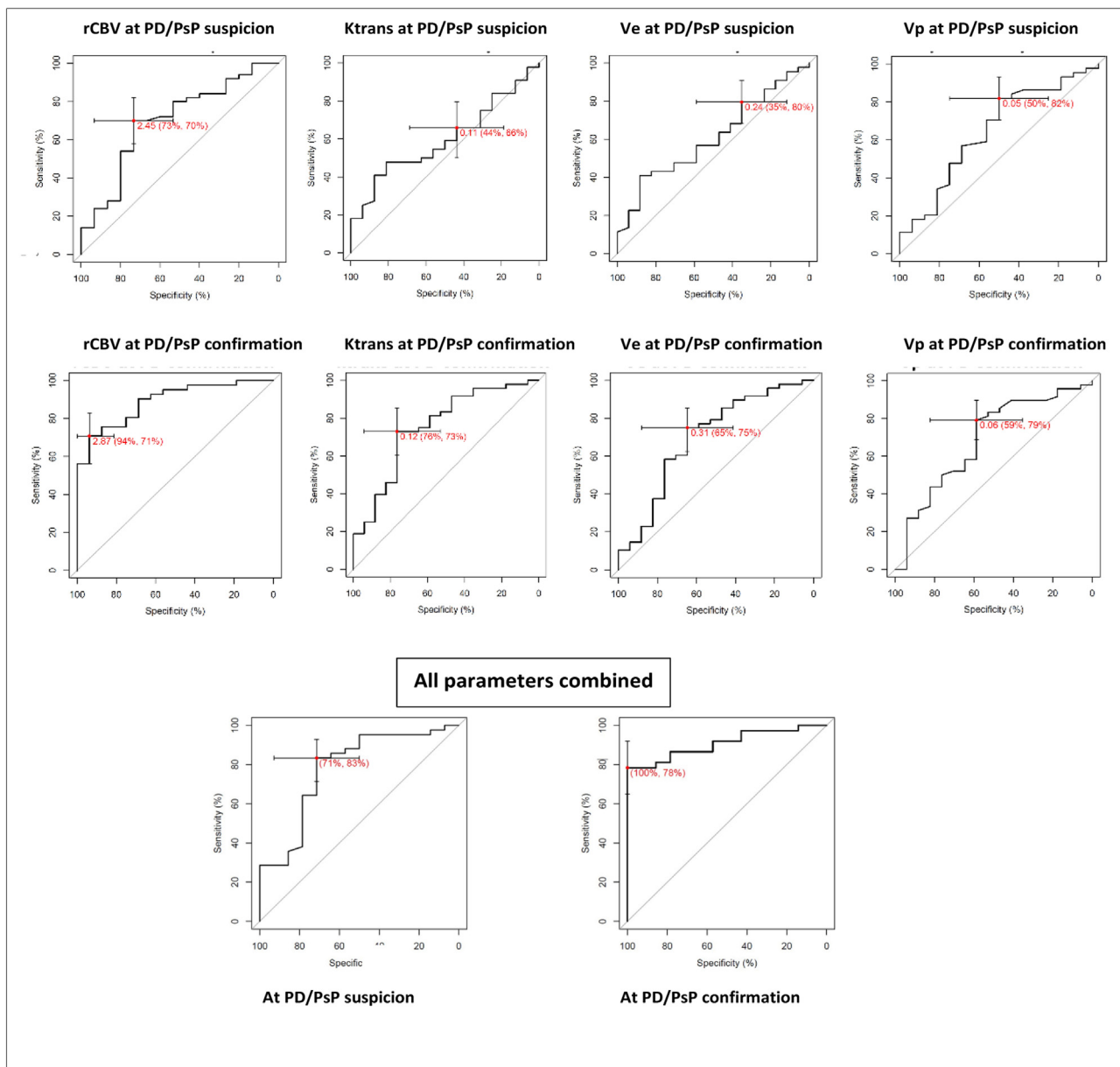


Fig. 2. Diagnostic accuracy and ROC curves for the multiparametric analysis including all four individual parameters rCBV, Ktrans, Ve and Vp and their combination at the first suspicion of progression (PD/PsP suspicion) and at the confirmation MRI (PD/PsP confirmation). (The values in red represent for the individual parameters the threshold values and the specificity and sensitivity and for the combination of parameters the specificity and sensitivity).

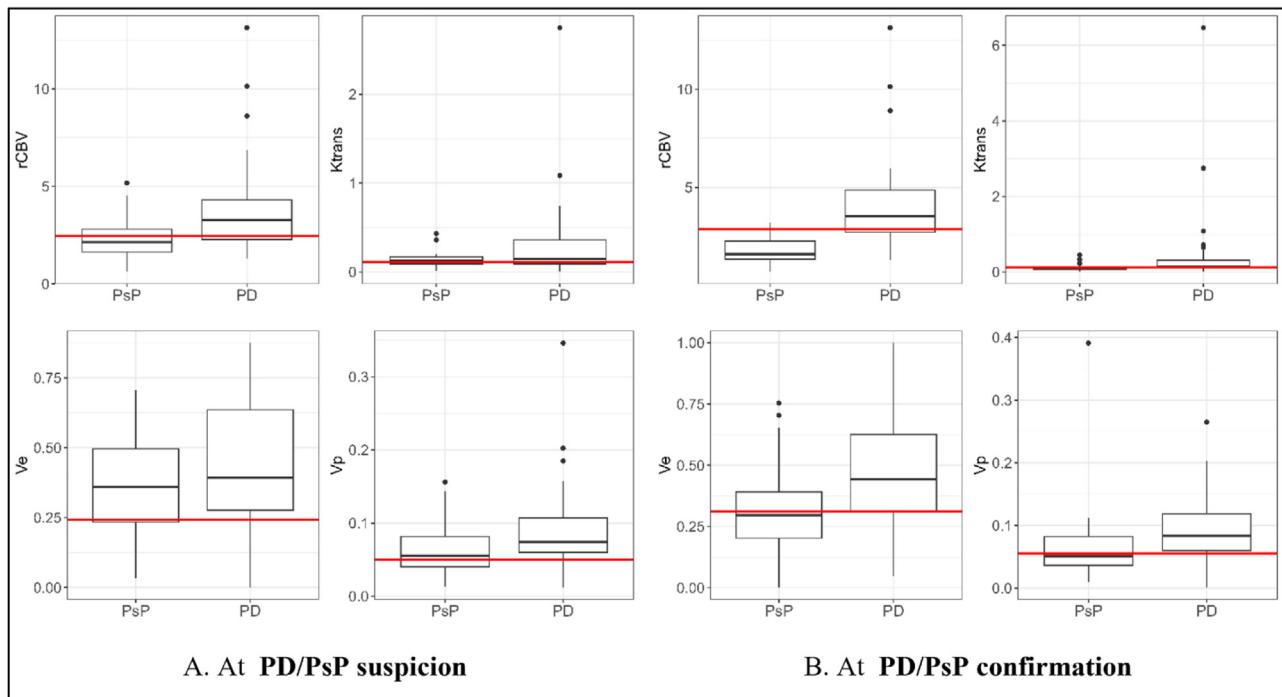


Fig. 3. Boxplots showing differences between the perfusion parameters in the PD and PsP group at the suspicion and at the confirmation MRI. The redline represents the best threshold value to distinguish PD from PsP.

Table 4
Mean threshold and mean AUC of the leave one out cross validation (LOOCV) at the PD/PsP suspicion and at the PD/PsP confirmation.

	Parameter	Threshold	AUC with CI
At the PD/PsP suspicion	rCBV	2.45	0.70 [0.68, 0.73]
	Ktrans	0.11	0.60 [0.58, 0.62]
	Ve	0.24	0.61 [0.59, 0.63]
	Vp	0.05	0.64 [0.62, 0.68]
At PD/PsP confirmation	rCBV	2.87	0.89 [0.88, 0.91]
	Ktrans	0.12	0.75 [0.74, 0.79]
	Ve	0.31	0.70 [0.68, 0.73]
	Vp	0.05	0.69 [0.67, 0.71]

above but also allows a simple qualitative visual assessment of the intralesional physiological changes through color-coded maps as showed in Figs. 4. and 5. Additionally, while not the subject in this study, the analysis of the signal intensity time-curve derived from DCE-MRI could further aid in differentiating PD from PsP.

In this study, the inter-reader reliability for rCBV was only fair, while it was excellent for Ktrans, underscoring the advantage of combining both techniques to reduce subjectivity. This combined approach might be particularly useful when rCBV values are close to the threshold or affected by technical limitations.

However, adding DCE-MRI to DSC-MRI increases acquisition time and may lead to patient intolerance, highlighting the need to balance diagnostic performance with feasibility. In patients - where the diagnostic gain is smaller and clinical context often guides decisions—a shorter protocol using only DSC-MRI may be sufficient.

In addition to evaluating the diagnostic accuracy of individual perfusion parameters—as reported in previous studies³⁵⁻³⁹—this study provides threshold values that may support radiologists in clinical decision-making. Although the sensitivity and specificity of individual parameters varied, the following thresholds may help distinguish PD from PsP in practice: rCBV 2.87 (Sensitivity 71 %, Specificity 94 %), Ktrans 0.12 min⁻¹ (Sensitivity 73 %, Specificity 76 %), Ve 0.31 (Sensitivity 75 %, Specificity 65 %), and Vp 0.05 (Sensitivity 78 %, Specificity 59 %) (Figs. 4 and 5).

A. Longitudinal MRI follow-up: diagnosis MRI, postoperative scan, and 2 consecutive MRI follow-up exams with a new and enlarging CE lesion suspicious for tumor progression in the irradiated volume within 12 weeks after RCT. PD is confirmed in two consecutive follow-ups after 12-weeks after completion of RCT and followed by a second resection with histologic and molecular confirmation of the tumor progression (upper row: axial Fluid attenuated inversion recovery (FLAIR) sequence, lower row: axial contrast enhanced T1weighted sequence, GTR: Gross total resection)

B. GRASP DCE-MRI and DSC-MRI parameters with persistent vascular phase in tumoral tissue: the color-coded maps of rCBV, Ktrans, Vp, Ve, and mean values of each parameter, indicate PD already within 12 weeks after RCT (rCBV > 2.8, Ktrans > 0.12 min⁻¹, Ve > 0.3, Vp > 0.05).

A. Serial MRI follow-up with stabilization of the lesion on the scans performed >9 months after the completion of RCT (upper row: axial TIRM sequence, lower row: axial contrast enhanced T1W sequence, GTR: Gross total resection). After 08/2021, the patient was under Bevacizumab therapy to control the edema around the pseudoprogression lesion.

B. GRASP DCE-MRI and DSC-MRI parameters: visual analysis of the color-coded maps show the absence of a vascular phase in the rCBV, Ktrans, Ve and Vp maps, and the mean values of each parameter also indicate pseudoprogression (rCBV < 2.8, Ktrans < 0.12 min⁻¹, Ve ≈ 0.3, Vp < 0.05).

The cut-off values obtained in this study for the commonly used perfusion parameters align with the ranges reported in the literature: rCBV values between 1.75 and 2.4³⁵⁻³⁸ and mean Ktrans at 0.08–0.19 min⁻¹ [38, 40].

Regarding the value of combining DSC- with DCE- derived perfusion parameters in one study from 2018, Nael et al.³⁸ showed that while rCBV outperforms Ktrans in distinguishing recurrent tumor from radiation necrosis, the combination of rCBV and Ktrans (thresholds 2.2 and 0.08 min⁻¹) may be used to improve the diagnostic accuracy in distinguishing PD from PsP to 93 %. Bisdas et al.⁴⁰ explored the value of Ktrans and Ve in predicting PD and found that the mean Ktrans was significantly higher in the recurrent glioma group than in the radiation necrosis group (p ≤ 0.0184) and they showed that a cutoff > 0.19 min⁻¹

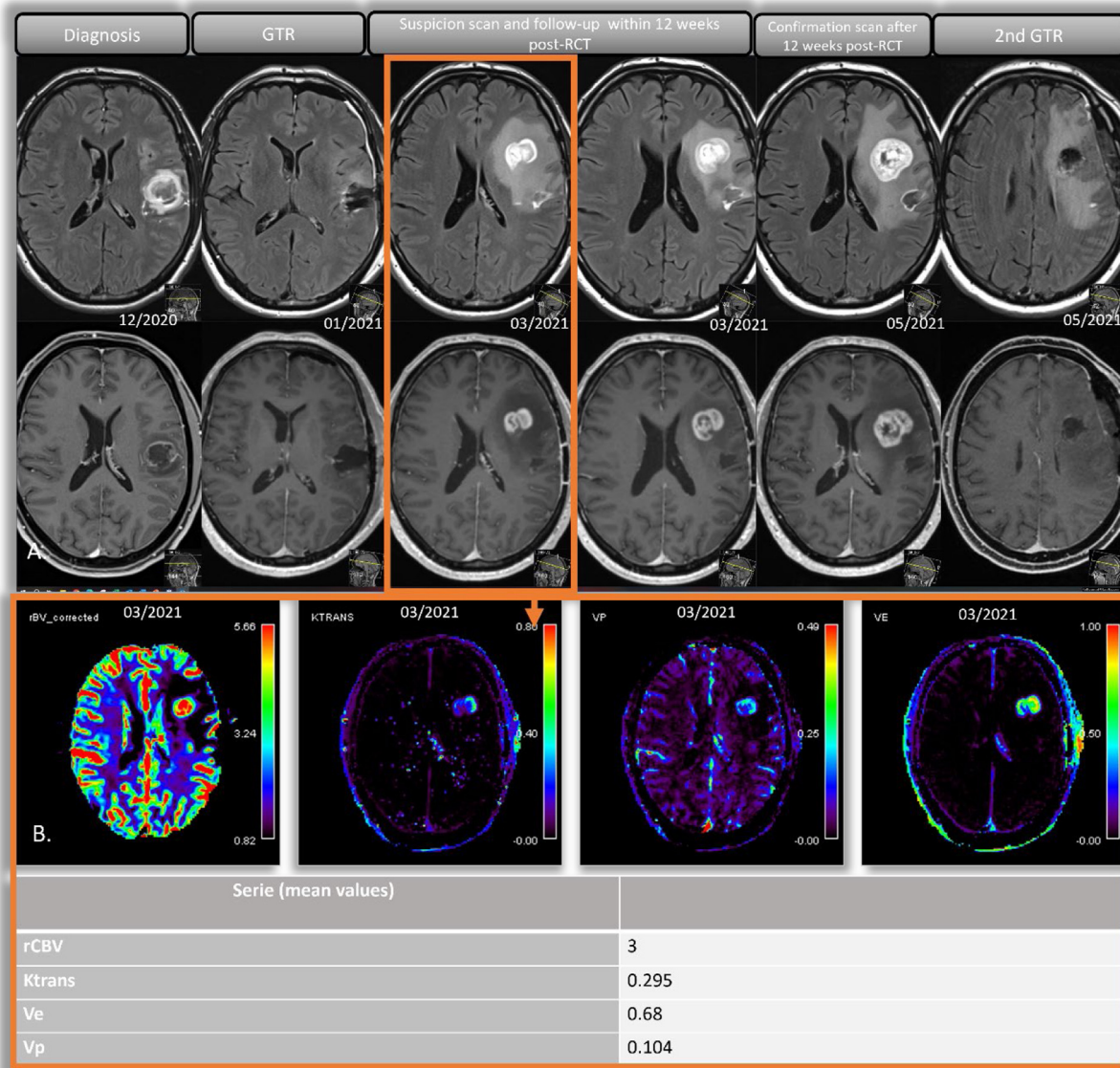


Fig. 4. Progressive disease within 12 weeks after completion of RCT in a 52-year-old male patient.

for Ktrans showed 100 % sensitivity and 83 % specificity for detecting recurrent gliomas. Like our findings, the Ve values were not significantly higher in recurrent tumors than those in radiation-induced necrotic lesions.

In our study, the median values of the perfusion parameters were generally higher in the PD group in comparison to the PsP group with rCBV (PD: 3.48 [2.49–4.84], PsP: 1.6 [1.33–2.27], $p < 0.001$) and Vp (PD: 0.08 [0.06–0.12], PsP: 0.05 [0.04–0.08], $p = .032$) showing statistically significant differences between groups. (Table 2). Given that both Vp and rCBV correlate with neovascularization density in brain tumors,^{41, 42} the ability to use Vp as an alternative to rCBV in cases where rCBV measurements are compromised by susceptibility artifacts represents a significant clinical advantage. As showed in a recent study³⁹ exploring the values of the longitudinal analysis of Ktrans and Vp, Vp gradually increased in the three scans prior to PD ($p = .0001$), suggesting it could be used not only as alternative to rCBV, but also as an early predictor of tumor progression.

One study conducted by Boxerman et al.,⁴² found no significant difference in the mean rCBV at initial progressive enhancement between PsP and PD (2.35 vs. 2.17; $p = .67$). However, he concluded that the longitudinal trend of rCBV (negative vs. positive slope; $p = .04$) may be

more effective in distinguishing PsP from PD than absolute values. While our study was not longitudinal, most MRIs indicating suspicion of progression were performed within 12 weeks post-radiochemotherapy, with confirmation scans primarily occurring more than 12 weeks post-radiochemotherapy. When looking at the values of the perfusion parameters, we have also observed a trend of higher median values in the PD group during the confirmation scans compared to the initial suspicion MRIs (Table 2), a finding that supports the hypothesis that a longitudinal follow up of the perfusion parameters may better differentiate PD from PsP than the absolute values at one single time-point after completion of RCT.

Other imaging techniques like FET-PET/CT and ASL (arterial spin labeling) have also proven high diagnostic accuracy in differentiating PD from PsP. Several studies showed that a TBRmax cut-off value of 2.3 can effectively distinguish PD from PsP with high specificity (100 %) and sensitivity (91 %).^{43, 44} Despite the high diagnostic accuracy of FET-PET/CT, we primarily use DSC- and DCE-MRI for glioblastoma follow-up in our routine practice, as they are more accessible, cost-effective, and do not require a radiotracer. FET-PET/CT is only used in unclear cases.

ASL has the advantage of not requiring gadolinium-based contrast agents, making it suitable for patients with contrast contraindications.⁴⁵

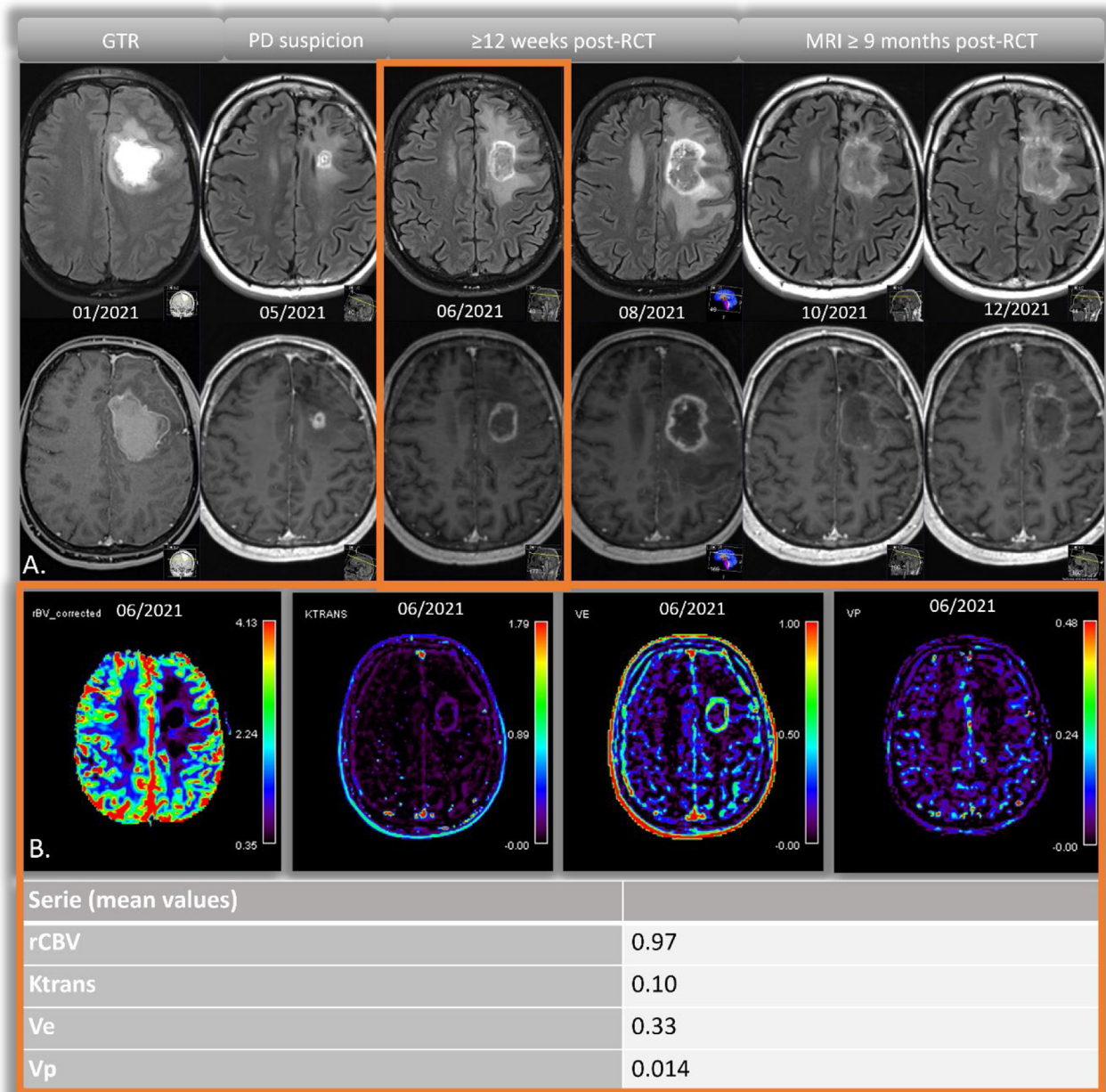


Fig. 5. Pseudoprogression 4 months after completion of concurrent RCT in a 44-year-old male patient.

Nevertheless, it has been shown that DSC-MRI provides better diagnostic accuracy compared to ASL, with DSC-MRI's sensitivity and specificity being 82.4 % and 67.9 %, respectively, versus ASL's 79.4 % and 64.3 %. The combination of both techniques improved sensitivity and specificity, but did not significantly enhance diagnostic accuracy.⁴⁶ Other studies have found comparable performance between 3D PCASL and DSC-MRI, with ASL showing higher AUC and less susceptibility to artifacts, particularly in areas like the skull base and adjacent to large resection cavities.⁴⁷ Despite these advantages, the longer acquisition time and lower signal-to-noise ratio of ASL limits its clinical implementation for monitoring treatment response in glioblastoma compared to DSC- and DCE-MRI.

The strengths of this study are the introduction of the GRASP technique in the assessment of treatment response in glioblastoma alongside DSC-MRI in one single protocol using a split-bolus technique, and the multiparametric analysis of the diagnostic accuracy of combined DSC-

and DCE-MRI parameters with their thresholds and the analysis at both suspicion of progression and the confirmation MRI.

GRASP DCE-MRI is an accelerated acquisition technique that provides high temporal and spatial resolution, enabling accurate estimation of pharmacokinetic parameters in tissues with rapid kinetics, such as glioblastoma.^{9, 18} The permeability parameters were measured with a temporal resolution of 4.3 s and a spatial resolution of $1.5 \times 1.5 \times 1.5$ mm³, consistent with the QIBA (Quantitative Imaging Biomarkers Alliance profile) recommendations, which suggest a temporal resolution of less than 10 s (ideally ≤ 5 s) for reliable estimation of Ktrans, Vp, and Ve.⁴⁸

The limitations of the study are the small sample size to validate the diagnostic performance of the thresholds for the different perfusion parameters in unseen data, as well as the imbalanced distribution of the number of patients and perfusion parameters between the PD and PsP group, which led to relatively wide confidence intervals for the

diagnostic accuracy of perfusion parameters and might limit the conclusions that can be drawn. To overcome this, we performed a leave-one-out cross validation analysis where we tested the stability of the thresholds for each perfusion parameter in each period. The AUC values obtained were very close to the ones in the main analysis; consequently, the results of the primary analysis were accepted as valuable. An ICC analysis between the two readers did show excellent reliability for Ktrans and good reliability for Ve, but only fair reliability for rCBV and poor reliability for Vp. The poor reliability for Vp might be explained by the very small absolute values observed for this parameter, reason why even minor variations in measurement can lead to large relative errors, reducing reliability.

To conclude, this study offers a detailed evaluation of the diagnostic accuracy of multiparametric analysis using a combined DSC- and GRASP DCE-MRI approach for assessing treatment response in glioblastoma patients. We identified optimal threshold values for key perfusion parameters to help differentiate between PD and PsP. Although exploratory, our findings provide meaningful guidance for neuroradiologists on integrating the double perfusion protocol into clinical practice. We also outlined the strengths and limitations of each technique and highlighted the clinical time points where their combined use is most advantageous. Nonetheless, larger, and more balanced prospective studies are needed to validate these results.

Conclusions

Combining DCE- with DSC-MRI may enhance diagnostic accuracy in distinguishing progressive disease from pseudoprogression in glioblastoma, particularly during the early post-radiochemotherapy phase when treatment decisions are critical. As the added value of DCE-MRI is limited beyond 12 weeks post-RCT, the full protocol is best reserved for early suspicion of progression or unclear cases, while DSC-MRI alone may be sufficient for confirmation imaging after this period.

Funding

The study was supported by an institutional grant offered in 2022 by the University of Basel Research Fund for Excellent Junior Researchers: Nr. 3MS1090. The corresponding author has benefitted of the grant.

Data availability

Data generated or analyzed during the study are available from the corresponding author by request.

Declaration of competing interest

The authors declare no conflicts of interest related to the content of this article.

Supplementary materials

Supplementary material associated with this article can be found in the online version at [doi:10.1016/j.neurad.2025.101354](https://doi.org/10.1016/j.neurad.2025.101354).

References

- Chen B, Chen C, Zhang Y, Xu J. Recent incidence trend of elderly patients with glioblastoma in the United States, 2000–2017. *BMC Cancer*. 2021;21(1):54.
- Louis DN, et al. The 2021 WHO classification of tumors of the central nervous system: a summary. *Neuro Oncol*. 2021;23(8):1231–1251.
- Schaff LR, Mellinghoff IK. Glioblastoma and other primary brain malignancies in adults: a review. *JAMA*. 2023;329(7):574–587.
- Hanif F, et al. Glioblastoma multiforme: a review of its epidemiology and pathogenesis through clinical presentation and treatment. *Asia Pac J Cancer Prev*. 2017;18(1):3–9.
- Stupp R, et al. Radiotherapy plus concomitant and adjuvant temozolomide for glioblastoma. *N Engl J Med*. 2005;352(10):987–996.
- Wen PY, et al. RANO 2.0: update to the response assessment in neuro-oncology criteria for high- and low-grade gliomas in adults. *J Clin Oncol*. 2023;41(33):5187–5199.
- Leao DJ, et al. Response assessment in neuro-oncology criteria for gliomas: practical approach using conventional and advanced techniques. *AJNR Am J Neuroradiol*. 2020;41(1):10–20.
- Thust SC, van den Bent MJ, Smits M. Pseudoprogression of brain tumors. *J Magnet Resonan Imaging*. 2018;48(3):571–589.
- van Dijken BRJ, et al. Perfusion MRI in treatment evaluation of glioblastomas: clinical relevance of current and future techniques. *J Magn Reson Imaging*. 2019;49(1):11–22.
- Cuenod CA, Balvay D. Perfusion and vascular permeability: basic concepts and measurement in DCE-CT and DCE-MRI. *Diagn Interv Imaging*. 2013;94(12):1187–1204.
- Henriksen OM, et al. High-grade glioma treatment response monitoring biomarkers: a position statement on the evidence supporting the use of advanced MRI techniques in the clinic, and the latest bench-to-bedside developments. Part 1: perfusion and diffusion techniques. *Front Oncol*. 2022:12.
- Bammer R, Amukotwa SA. Dynamic Susceptibility Contrast Perfusion, Part 1: The Fundamentals. *Magn Reson Imaging Clin N Am*. 2024;32(1):1–23.
- Lee J, et al. MR perfusion imaging for gliomas. *Magn Reson Imaging Clin N Am*. 2024;32(1):73–83.
- van Dijken BRJ, et al. Perfusion MRI in treatment evaluation of glioblastomas: Clinical relevance of current and future techniques. *J Magnet Reson Imaging*. 2019;49(1):11–22.
- Kimura M, da Cruz LCH. Multiparametric MR imaging in the assessment of brain tumors. *Magn Reson Imaging Clin N Am*. 2016;24(1):87–122.
- Østergaard L. Principles of cerebral perfusion imaging by bolus tracking. *J Magn Reson Imaging*. 2005;22(6):710–717.
- van Dijken BRJ, van Laar PJ, Holtman GA, van der Hoorn A. Diagnostic accuracy of magnetic resonance imaging techniques for treatment response evaluation in patients with high-grade glioma, a systematic review and meta-analysis. *Eur Radiol*. 2017;27(10):4129–4144.
- Li X, Huang W, Holmes JH. Dynamic Contrast-Enhanced (DCE) MRI. *Magn Reson Imaging Clin N Am*. 2024;32(1):47–61.
- Zakhari N, et al. Prospective comparative diagnostic accuracy evaluation of dynamic contrast-enhanced (DCE) vs. dynamic susceptibility contrast (DSC) MR perfusion in differentiating tumor recurrence from radiation necrosis in treated high-grade gliomas. *J Magnet Reson Imaging*. 2019;50(2):573–582.
- Feng L, et al. Golden-angle radial sparse parallel MRI: combination of compressed sensing, parallel imaging, and golden-angle radial sampling for fast and flexible dynamic volumetric MRI. *Magn Reson Med*. 2014;72(3):707–717.
- Feng L, et al. Magnetization-prepared GRASP MRI for rapid 3D T1 mapping and fat/water-separated T1 mapping. *Magn Reson Med*. 2021;86(1):97–114.
- Benz MR, et al. Acceleration techniques and their impact on arterial input function sampling: Non-accelerated versus view-sharing and compressed sensing sequences. *Eur J Radiol*. 2018;104:8–13.
- Singh D, et al. Emerging trends in fast MRI using deep-learning reconstruction on undersampled k-space data: a systematic review. *Bioeng (Basel)*. 2023;(9):10.
- Leu K, Boxerman JL, Ellingson BM. Effects of MRI protocol parameters, preload injection dose, fractionation strategies, and leakage correction algorithms on the fidelity of dynamic-susceptibility contrast MRI estimates of relative cerebral blood volume in gliomas. *AJNR Am J Neuroradiol*. 2017;38(3):478–484.
- Harris PA, et al. The REDCap consortium: building an international community of software platform partners. *J Biomed Inform*. 2019;95:103208.
- Feng L. Golden-angle radial MRI: basics, advances, and applications. *J Magnet Reson Imaging*. 2022;56(1):45–62.
- Olea, User Guide Olea Sphere 2.2 <http://190.254.50.74/vital/help/en/pdf/Olea-Sphere20User20Guide20v2.2.pdf>. 2012.
- DeLong ER, DeLong DM, Clarke-Pearson DL. Comparing the areas under two or more correlated receiver operating characteristic curves: a nonparametric approach. *Biometrics*. 1988;44(3):837–845.
- Fawcett T. An introduction to ROC analysis. *Patt Recognit Lett*. 2006;27(8):861–874.
- Blaker H. Confidence curves and improved exact confidence intervals for discrete distributions. *Canad J Statist/La Revue Canadienne de Statistique*. 2000;28(4):783–798.
- Sun X, Xu W. Fast implementation of DeLong's algorithm for comparing the areas under correlated receiver operating characteristic curves. *IEEE Signal Process Lett*. 2014;21(11):1389–1393.
- Robin X, et al. pROC: an open-source package for R and S+ to analyze and compare ROC curves. *BMC Bioinform*. 2011;12:77.
- Brandsma D, van den Bent MJ. Pseudoprogression and pseudoresponse in the treatment of gliomas. *Curr Opin Neurol*. 2009;22(6):633–638.
- Hygino da Cruz Jr. LC, et al. Pseudoprogression and pseudoresponse: imaging challenges in the assessment of posttreatment glioma. *AJNR Am J Neuroradiol*. 2011;32(11):1978–1985.
- Anil A, et al. Identification of single-dose, dual-echo based CBV threshold for fractional tumor burden mapping in recurrent glioblastoma. *Front Oncol*. 2023;13:1046629.
- Kuo F, et al. DSC perfusion MRI-derived fractional tumor burden and relative CBV differentiate tumor progression and radiation necrosis in brain metastases treated with stereotactic radiosurgery. *Am J Neuroradiol*. 2022;43(5):689–695.
- Nierobisch N, et al. Comparison of clinically available dynamic susceptibility contrast post processing software to differentiate progression from pseudoprogression in post-treatment high grade glioma. *Eur J Radiol*. 2023;167:111076.
- Nael K, et al. Multiparametric MRI for differentiation of radiation necrosis from recurrent tumor in patients with treated glioblastoma. *AJR Am J Roentgenol*. 2018;210(1):18–23.

39. Arevalo-Perez J, et al. Longitudinal evaluation of DCE-MRI as an early indicator of progression after standard therapy in glioblastoma. *Cancer (Basel)*. 2024;16(10):1839.
40. Bisdas S, et al. Distinguishing recurrent high-grade gliomas from radiation injury: a pilot study using dynamic contrast-enhanced MR imaging. *Acad Radiol*. 2011;18(5):575–583.
41. Mills SJ, et al. Enhancing fraction in glioma and its relationship to the tumoral vascular microenvironment: a dynamic contrast-enhanced MR imaging study. *Am J Neuroradiol*. 2010;31(4):726–731.
42. Boxerman JL, et al. Longitudinal DSC-MRI for distinguishing tumor recurrence from pseudoprogression in patients with a high-grade glioma. *Am J Clin Oncol*. 2017;40(3):228–234.
43. Galldiks N, et al. Diagnosis of pseudoprogression in patients with glioblastoma using O-(2-[18F]fluoroethyl)-l-tyrosine PET. *Eur J Nucl Med Mol Imaging*. 2015;42(5):685–695.
44. Puranik AD, et al. FET PET to differentiate between post-treatment changes and recurrence in high-grade gliomas: a single center multidisciplinary clinic controlled study. *Neuroradiology*. 2024.
45. Taylor C, et al. Discriminators of pseudoprogression and true progression in high-grade gliomas: A systematic review and meta-analysis. *Sci Rep*. 2022;12(1):13258.
46. Choi YJ, et al. Pseudoprogression in patients with glioblastoma: added value of arterial spin labeling to dynamic susceptibility contrast perfusion MR imaging. *Acta Radiol*. 2013;54(4):448–454.
47. Manning P, et al. Differentiation of progressive disease from pseudoprogression using 3D PCASL and DSC perfusion MRI in patients with glioblastoma. *J Neurooncol*. 2020;147(3):681–690.
48. QIBA Profile: DCE-MRI Quantification (DCEMRI-Q). http://qibawiki.rsna.org/images/1/1f/QIBA_DCE-MRI_Profile-Stage_1-Public_Comment.pdf 2017.